

## Highlights from BESIII experiment

Yanping Huang<sup>a</sup> on behalf of the BESIII Collaboration

Institute of High Energy Physics Beijing 100049, China

**Abstract.** BESIII had collected large data samples on  $J/\psi$  and  $\psi'$  peaks during the first run in 2009. We review recent results on charmonium decays and hadron spectroscopy. The prospects on open charm physics are also discussed.

### 1 Introduction

The newly built BEPCII/BESIII is an upgrade to the previous BEPC/BES [1]. The BEPCII is a double ring collider with a design luminosity of  $1 \times 10^{33} \text{cm}^{-2} \text{s}^{-1}$  at a center-of-mass energy of 3.78 GeV, which luminosity is one order of higher than that at CESR-c. It is operating between 2.0 and 4.6 GeV in the center of mass. The BESIII experiment is used to study the charm and  $\tau$  physics. It is foreseen to collect on the order of 10 billion  $J/\psi$  events or 3 billion  $\psi(2S)$  events per year according to the designed luminosity. About 32 million  $D\bar{D}$  pairs and 2.0 million  $D_S\bar{D}_S$  at threshold will be collected per year [1]. In last run, the peak luminosity of BEPCII has reached  $6.5 \times 10^{32} \text{cm}^{-2} \text{s}^{-1}$ .

In 2009, the BESIII had collected about 225 M and 106M data set on the  $J/\psi$  and  $\psi'$  peaks, respectively. The results in this paper is based above data set.

### 2 Highlights from BESIII

The BESIII collaboration has published so-far a variety of papers with many new results in the field of light hadron and charmonium spectroscopy, as well as charmonium decays [2–12]. A number of new hadronic states were discovered or confirmed, and various decay properties were measured for the first time. In addition, many data analyses are in an advanced stage and will lead to a rich set of new publications in the near future. Here, we show recent highlights from the BESIII, thereby, illustrating the potential of the BESIII experiment. In this paper, for the reported experimental results, the first error and second error will be statistical and systematic, respectively, if they are not specified.

#### 2.1 $\eta_c(1S)$ resonance via $\psi' \rightarrow \gamma\eta_c$ decay

Based on the data sample of 106 M  $\psi'$  events collected with BESIII detector, the  $\eta_c$  mass and width are measured from the radiative transition  $\psi' \rightarrow \gamma\eta_c$ . The  $\eta_c$  candidates are reconstructed from six exclusive decay modes:  $K_S K\pi$ ,  $K^+ K^- \pi^0$ ,  $\eta\pi^+\pi^-$ ,  $K_S K^+ \pi^- \pi^+\pi^-$ ,  $K^+ K^- \pi^+\pi^- \pi^0$ , and  $3(\pi^+\pi^-)$ , where  $K_S$  is reconstructed in  $\pi^+\pi^-$  mode,  $\eta$  and  $\pi^0$  from  $\gamma\gamma$  final states. For a hindered M1 transition the matrix element acquires terms proportional to  $E_\gamma^2$ , which, when combined with the usual  $E_\gamma^3$  term for the allowed transitions, lead to contributions in the radiative width proportional to  $E_\gamma^7$ . Thus, the  $\eta_c$  lineshape is described by a BW modified by  $E_\gamma^7$  convoluted with a resolution function. It is important to point out that the interference between  $\eta_c$  and non-resonance in the signal region is also

<sup>a</sup> e-mail: huangyp@ihep.ac.cn

considered. The statistical significance of the interference is  $15\sigma$ . This affects the  $\eta_c$  resonant parameters significantly. Assuming an universal relative phase between the two amplitudes, we obtain  $\eta_c$  mass and width,  $M = 2984.2 \pm 0.6 \pm 0.5 \text{ MeV}/c^2$  and  $\Gamma = 31.4 \pm 1.2 \pm 0.6 \text{ MeV}$ , respectively, as well as the relative phase  $\phi = 2.41 \pm 0.06 \pm 0.04 \text{ rad}$ . Figure 1 shows the fit results in the six  $\eta_c$  decay modes. With precise measurement of the  $\eta_c$  mass, one can obtain the hyperfine splitting,  $\Delta M_{hf}(1S)_{c\bar{c}} \equiv M(J/\psi) - M(\eta_c) = 112.5 \pm 0.8 \text{ MeV}$ , which agrees with the quark model prediction [14], and will be helpful for understanding the spin-dependent interactions in hidden quarkonium states.

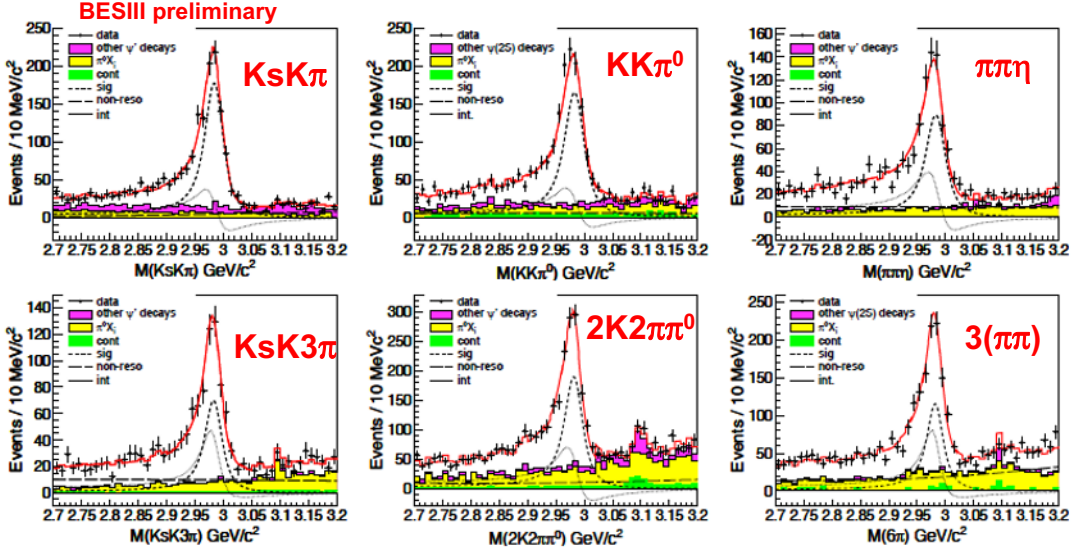


**Fig. 1.** The invariant mass distributions for the decays  $K_s K \pi$ ,  $K^+ K^- \pi^0$ ,  $\eta \pi^+ \pi^-$ ,  $K_s K^+ \pi^- \pi^+ \pi^-$ ,  $K^+ K^- \pi^+ \pi^- \pi^0$ , and  $3(\pi^+ \pi^-)$ , respectively. Solid curves show the fitting results; the fitting components ( $\eta_c$  signal/non-resonance/interference) are shown as (dashed/long-dashed/dotted) curves. Points with error bar are data, shaded histograms are (in green/yellow/magenta) for (continuum/other  $\eta_c$  decays/other  $\psi'$  decays) backgrounds.

## 2.2 Observation of $\psi' \rightarrow \gamma \eta_c(2S)$

Using the largest  $\psi'$  data sample in the world which was collected by the BESIII, we searched for the M1 transition  $\psi' \rightarrow \gamma \eta_c(2S)$  through the hadronic final states  $K_s K^\pm \pi^\mp$ . A bump is observed around 3635 MeV on the mass spectrum as shown in Fig. 2. In order to determine the background and mass resolution using data, the mass spectrum range is enlarged ( $3.47 \sim 3.72 \text{ GeV}/c^2$ ) to include  $\chi_{c1}$  and  $\chi_{c2}$  events. The resonances  $\chi_{c1}$  and  $\chi_{c2}$  are described by the corresponding Monte Carlo (MC) shape convolved a Gaussian which takes account the small difference on the mass shift and resolution between data and MC. So the mass resolution for the  $\eta_c(2S)$  in the fitting is fixed to the linear extrapolation of the mass resolutions from the  $\chi_{c1}$  and  $\chi_{c2}$  signals in data. The line shape for  $\eta_c(2S)$  produced by such the M1 transition is described by  $(E_\gamma^3 \times BW(m) \times \text{damping}(E_\gamma)) \otimes \text{Gauss}(0, \sigma)$  where  $m$  is the invariant mass of  $K_s K^\pm \pi^\mp$ ,  $E_\gamma = \frac{m_{\psi'}^2 - m^2}{2m_{\psi'}}$  is the energy of the transition photon in the rest frame of  $\psi'$ ,  $\text{damping}(E_\gamma)$  is the function to damp the diverging tail raised by  $E_\gamma^3$  and  $\text{Gauss}(0, \sigma)$  is the Gaussian function describing the detector resolution. In the fit, the width of  $\eta_c(2S)$  is fixed to PDG value. From the fit to the data, a signal with a statistical significance of 6.5 standard deviation is observed which is the first observation of the M1 transition  $\psi' \rightarrow \gamma \eta_c(2S)$ . The mea-

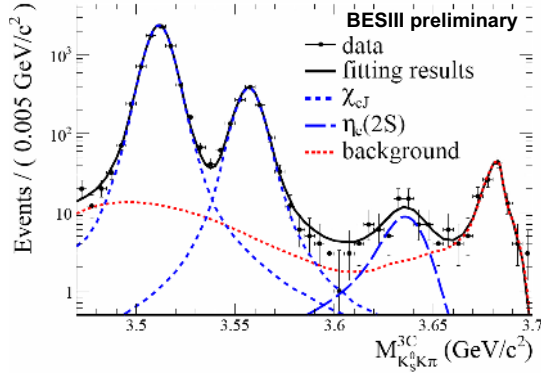


Fig. 2. Fitting of the mass spectrum for  $\eta_c(2S) \rightarrow K_s K^\pm \pi^\mp$ .

sured mass for  $\eta_c(2S)$  is  $3638.5 \pm 2.3 \pm 1.0$  MeV/ $c^2$ . The measured branching ratio is  $BR(\psi' \rightarrow \gamma \eta_c(2S)) \times BR(\eta_c(2S) \rightarrow K_s K^\pm \pi^\mp) = (2.98 \pm 0.57 \pm 0.48) \times 10^{-6}$ . Together with the BABAR result  $BR(\eta_c(2S) \rightarrow K \bar{K} \pi) = (1.9 \pm 0.4 \pm 1.1)\%$  [15], the M1 transition rate for  $\psi' \rightarrow \gamma \eta_c(2S)$  is derived as  $BR(\psi' \rightarrow \gamma \eta_c(2S)) = (4.7 \pm 0.9 \pm 3.0) \times 10^{-4}$ .

### 2.3 $h_c(1P)$ properties

The BESIII Collaboration reported the results on the production and decay of the  $h_c$  using 106M of  $\psi'$  decay events in 2010 [2], where we studied the distributions of mass recoiling against a detected  $\pi^0$  to measure  $\psi' \rightarrow \pi^0 h_c$  both inclusively (E1-untagged) and in events tagged as  $h_c \rightarrow \gamma \eta_c$  (E1-tagged) by detection of the E1 transition photon. In 2011, 16 specific decay modes of  $\eta_c$  are used to reconstruct  $\eta_c$  candidates in the decay mode of  $h_c \rightarrow \gamma \eta_c$ . Fig. 3 is the sum of the 16 decay modes. We fit the 16  $\pi^0$  recoil-mass spectra simultaneously that yields  $M(h_c) = 3525.31 \pm 0.11(stat.) \pm 0.15(syst.)$  MeV/ $c^2$  and  $\Gamma(h_c) = 0.70 \pm 0.28(stat.) \pm 0.25(syst.)$  MeV/ $c^2$ . These preliminary results are consistent with the previous BESIII inclusive results and CLEO-c exclusive results.

The centroid of the  $^3P_J$  states ( $\chi_{c0}, \chi_{c1}, \chi_{c2}$ ) is known to be  $\langle M(^3P_J) \rangle = [5M(^3P_2) + 3M(^3P_1) + M(^3P_0)] = 3525.30 \pm 0.04$  MeV [13]. If the  $^3P_J$  states centroid mass  $\langle M(^3P_J) \rangle$  is identified as the mass of  $M(^3P)$ , then BESIII observes the hyperfine splitting as  $\Delta M_{hf}(1P)_{cc} = -0.01 \pm 0.11(stat.) \pm 0.14(syst.)$  MeV which agrees with zero.

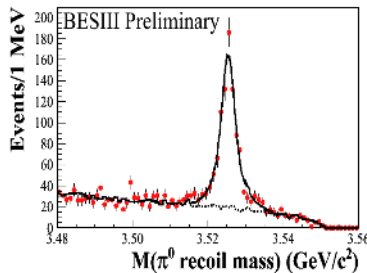
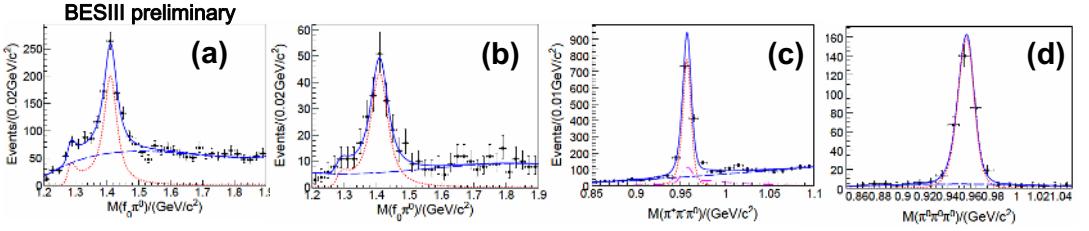


Fig. 3. The  $\pi^0$  recoiling mass for the sum of 16  $\eta_c$  decay modes.



**Fig. 4.** The invariant mass distributions: (a) invariant mass of  $f_0(980)\pi^0$  from  $J/\psi \rightarrow \gamma\pi^+\pi^-\pi^0$ ; (b) invariant mass of  $f_0(980)\pi^0$  mass from  $J/\psi \rightarrow \gamma\pi^0\pi^0\pi^0$ ; (c) the invariant mass of  $\eta' \rightarrow 3\pi$ s in  $J/\psi \rightarrow \gamma\pi^+\pi^-\pi^0$ , (d) mass of  $\eta' \rightarrow 3\pi$ s from  $J/\psi \rightarrow \gamma\pi^0\pi^0\pi^0$ , respectively.

## 2.4 $\eta'$ and $\eta(1405)$ in $J/\psi \rightarrow \gamma\pi\pi\pi$ decays

The spectrum of radial excitation states of isoscalar  $\eta$  and  $\eta'$  is still not well known. An important issue is about the nature of  $\eta(1405)$  and  $\eta(1475)$  states, which are not well established. BESIII measured the decays of  $J/\psi \rightarrow \gamma\pi^+\pi^-\pi^0$  and  $\gamma\pi^0\pi^0\pi^0$ . In the two decay modes, clear  $f_0(980)$  signals are observed on both  $\pi^+\pi^-$  and  $\pi^0\pi^0$  spectra, the width of observed  $f_0(980)$  is much narrower ( $\sim 10$  MeV) than that in other processes [13]. By taking events in the window of  $f_0(980)$  on the  $\pi\pi$  mass spectrum, we observed evidence of  $f_1(1285)$  in the low mass region of  $f_0(980)\pi^0$  as shown in Fig. 4 (a) and (b), which corresponding to significance of about  $4.8\sigma$  for  $f_1(1285) \rightarrow f_0(980)\pi^0$  in  $f_0(980) \rightarrow \pi^+\pi^-$  mode ( $1.4\sigma$  in  $f_0(980) \rightarrow \pi^0\pi^0$ ). It is interesting that clear peak around 1400 MeV is also observed on the mass of  $f_0(980)\pi^0$  (see Fig. 4 (a) and (b)). Preliminary angular analysis indicates that the peak on 1400 MeV is from  $\eta(1405) \rightarrow f_0(980)\pi^0$  decay. BESIII measured the combined branching fraction of  $\eta(1405)$  production to be  $BR(J/\psi \rightarrow \gamma\eta(1405)) \times BR(\eta(1405) \rightarrow f_0(980)\pi^0) \times BR(f_0(980) \rightarrow \pi^+\pi^-) = (1.48 \pm 0.13 \pm 0.17) \times 10^{-5}$  and  $BR(J/\psi \rightarrow \gamma\eta(1405)) \times BR(\eta(1405) \rightarrow f_0(980)\pi^0) \times BR(f_0(980) \rightarrow \pi^0\pi^0) = (6.99 \pm 0.93 \pm 0.95) \times 10^{-6}$ , respectively. It is the first time that we observe anomalously large isospin violation in the strong decay of  $\eta(1405) \rightarrow f_0(980)\pi^0$ .

By looking at the invariant mass of  $\pi\pi\pi$  in  $J/\psi \rightarrow \gamma 3\pi$ s decays as shown in Fig. 4 (c) and (d), we observe signals for  $\eta' \rightarrow \pi^+\pi^-\pi^0$  and  $\pi^0\pi^0\pi^0$  decays, respectively, and determine the decay rates to be  $BR(\eta' \rightarrow \pi^+\pi^-\pi^0) = (3.83 \pm 0.15 \pm 0.39) \times 10^{-3}$  and  $BR(\eta' \rightarrow \pi^0\pi^0\pi^0) = (3.56 \pm 0.22 \pm 0.34) \times 10^{-3}$ , respectively. For  $\eta' \rightarrow \pi^+\pi^-\pi^0$  decay, it is consistent with CLEO-c's measurements and precision is improved by a factor of 4. In contrast, for  $\eta' \rightarrow \pi^0\pi^0\pi^0$  decay, it is two times larger than that in the PDG value [13].

## 2.5 Observation of $\pi^+\pi^-$ resonances above 2.0 GeV in $J/\psi \rightarrow \gamma\eta'\pi^+\pi^-$ decay

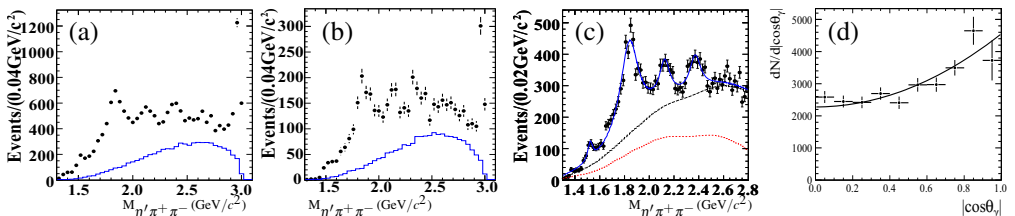


**Fig. 5.** The invariant mass distributions of  $\eta'\pi^+\pi^-$  with (a)  $\eta' \rightarrow \gamma\rho$  (b)  $\eta' \rightarrow \eta\pi^+\pi^-$ , and (c) the combined plot for (a) and (b), and fitting results. (d) is for the  $\cos(\theta_\gamma)$  distribution, where  $\theta_\gamma$  is the pole angle of the radiative photon. The points with error bar are data. The histograms are from  $J/\psi \rightarrow \gamma\eta'\pi^+\pi^-$  phase space MC.

The  $X(1835)$  was firstly observed at the BESII with a statistical significance of  $7.7\sigma$  [16]. The possible interpretations of the  $X(1835)$  include a  $p\bar{p}$  bound state [17,18], a glueball [19], a radial excitation of the  $\eta'$  meson [20], etc. We report a study of  $J/\psi \rightarrow \gamma\eta'\pi^+\pi^-$  that used two  $\eta'$  decay modes,  $\eta' \rightarrow \gamma\rho$  and  $\eta' \rightarrow \pi^+\pi^-\eta$ . Figure 5 (a) and (b) show the  $\eta'\pi^+\pi^-$  invariant mass spectrum in  $J/\psi \rightarrow \gamma\eta'\pi^+\pi^-$  with  $\eta' \rightarrow \gamma\rho$  and  $\eta' \rightarrow \pi^+\pi^-\eta$  decay modes, respectively. The  $X(1835)$  resonance is clearly seen. Additional peaks are observed around 2.1 and 2.3  $\text{GeV}/c^2$ , denoted as  $X(2120)$  and  $X(2370)$ , as well as the  $f_1(1510)$  in the low mass region and the distinct  $\eta_c(1S)$  signal in the high mass region.

Fits to the mass spectra have been made using four efficiency-corrected Breit-Wigner functions convolved with a Gaussian mass resolution plus a nonresonant  $\pi^+\pi^-\eta'$  contribution and background representations. The fitting result of the combined mass spectrum is shown in Fig. 5(c). The mass and width of  $X(1835)$  are measured to be  $M = 1836.5 \pm 3.0^{+5.6}_{-2.1} \text{ MeV}/c^2$  and  $\Gamma = 190 \pm 9^{+38}_{-36} \text{ MeV}$  with a significance larger than  $20\sigma$ . The mass and width for  $X(2120)$  ( $X(2370)$ ) is determined to be  $M = 2122.4 \pm 6.7^{+4.7}_{-2.7} \text{ MeV}/c^2$  ( $M = 2376.3 \pm 8.7^{+3.2}_{-4.3} \text{ MeV}/c^2$ ) and  $\Gamma = 83 \pm 16^{+31}_{-11} \text{ MeV}$  ( $\Gamma = 83 \pm 17^{+44}_{-6} \text{ MeV}$ ) with significance  $7.2\sigma$  ( $6.4\sigma$ ). For  $X(1835)$ , the  $\cos\theta_\gamma$  distribution is shown in Fig. 5, where  $\theta_\gamma$  is the polar angle of the radiative photon in the  $J/\psi$  center of mass system. It agrees with  $(1 + \cos^2\theta_\gamma)$ , which is expected for a pseudoscalar.

## 2.6 $p\bar{p}$ mass threshold enhancement in $J/\psi$ and $\psi'$ radiative decay

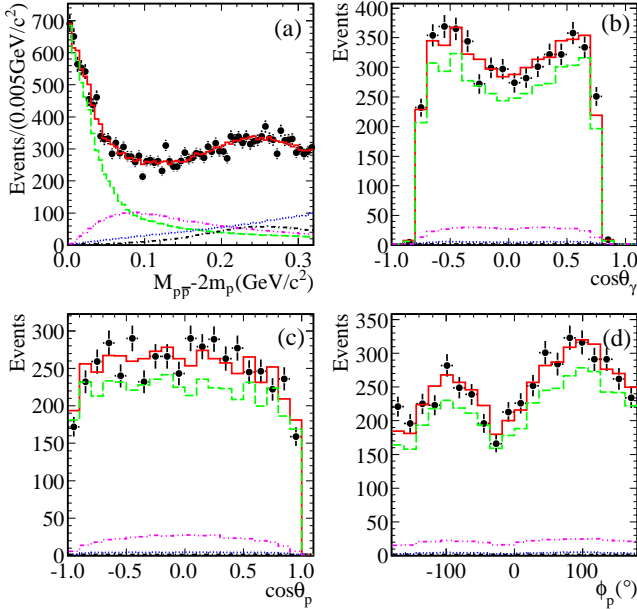


**Fig. 6.** Comparisons between data and PWA fit projection: (a) the  $p\bar{p}$  invariant mass; (b)-(d) the polar angle  $\theta_\gamma$  of the radiative photon in the  $J/\psi$  center of mass system, the polar angle  $\theta_p$  and the azimuthal angle  $\phi_p$  of the proton in the  $p\bar{p}$  center of mass system with  $M_{p\bar{p}} - 2m_p < 50 \text{ MeV}/c^2$ , respectively. Here, the black dots with error bars are data, the solid histograms show the PWA total projection, and the dashed, dotted, dash-dotted and dash-dot-dotted lines show the contributions of the  $X(p\bar{p})$ ,  $0^{++}$  phase space,  $f_0(2100)$  and  $f_2(1910)$ , respectively.

A partial wave analysis of the  $p\bar{p}$  mass-threshold enhancement in the reaction  $J/\psi \rightarrow \gamma p\bar{p}$  is used to determine: its  $J^{PC}$  quantum numbers to be  $0^{++}$ ; its peak mass to be below threshold at  $M =$

$1832_{-5}^{+19}$  (stat.) $_{-17}^{+18}$  (syst.)  $\pm 19$  (model) MeV/ $c^2$ ; and its total width to be  $\Gamma < 76$  MeV/ $c^2$  at the 90% C.L. The product of branching ratios is measured to be  $BR(J/\psi \rightarrow \gamma X(p\bar{p}))BR(X(p\bar{p}) \rightarrow p\bar{p}) = (9.0_{-1.1}^{+0.4}$  (stat.) $_{-5.0}^{+1.5}$  (syst.)  $\pm 2.3$  (model))  $\times 10^{-5}$ . A similar analysis performed on  $\psi(3686) \rightarrow \gamma p\bar{p}$  decays shows, for the first time, the presence of a corresponding enhancement with a production rate relative to that for  $J/\psi$  decays of  $R = (5.08_{-0.45}^{+0.71}$  (stat.) $_{-3.58}^{+0.67}$  (syst.)  $\pm 0.12$  (model))%.

## 2.7 Open charm physics

As of May, 2011, the BESIII has accumulated integrated luminosity of  $2.9 \text{ fb}^{-f}$  on  $\psi(3770)$  peak for open charm physics, which is about 3.5 times the previous largest  $\psi(3770)$  data set taken by the CLEO-c Experiment. Taking advantage of the high luminosity provided by the BEPCII collider, BESIII is expected to take much more data at both 3770 MeV and higher energies. Many high precision measurements, including CKM matrix elements related to charm weak decays, decay constants  $f_D$  and  $f_{D_s}$ , form factors from D semileptonic decays, Dalitz decays, searches for  $CP$  violation, and absolute decay branching fractions, will be accomplished in the near future.

There are many advantages of doing charm physics at experiments with  $e^+e^-$  collider at threshold. With  $e^+e^-$  colliding, the initial energy and quantum numbers are known. For  $\psi(3770) \rightarrow D\bar{D}$ , both D daughter mesons can be fully reconstructed, allowing absolute measurements, namely, the so called double-tag technique. The continuum background is greatly suppressed by doing this, and kinematic constraints can be applied to infer missing particles on the other side D meson. The neutrino can be reconstructed in the leptonic and semileptonic D decays, so that decay constants and form factor/CKM matrix elements can be precisely measured. Thus, these precise measurements could be used to test and calibrate the theoretical tools such as lattice QCD, which are critical for dealing with B decays.

## 3 Summary

The BESIII experiment addresses a wide range of topics in the field of QCD and searches for new physics beyond the standard model. At present the BESIII collaboration has collected a record on statistics on  $J/\psi$ ,  $\psi'$ , and  $\psi(3770)$  charmonium states. These data are being exploited to provide precision measurements with a high discovery potential in light hadron and charmonium spectroscopy, charmonium decays, and open charm productions. Most recent highlights from BESIII are reviewed in this paper.

Since very recently, data about  $470 \text{ pb}^{-1}$  luminosity have been taken at a center-of-mass energy of 4010 GeV, which could give new insights in our understanding of the recently discovered XYZ states and which will allow to explore the field of  $D_s$  physics.

We would like to thank the accelerator people at BEPCII for their hard work which makes our high luminosity possible. We would also like to thank the great computational and software support of the IHEP staff. This work is supported in part by the Ministry of Science and Technology of China.

## References

1. M. Ablikim *et al.* (BESIII Collaboration), Nucl. Instrum. Meth. **A614**, 345 (2009).
2. M. Ablikim *et al.* (BESIII Collaboration), Phys. Rev. Lett. **104**, 132002 (2010).
3. M. Ablikim *et al.* (BESIII Collaboration), Phys. Rev. Lett. **105**, 261801 (2010).
4. M. Ablikim *et al.* (BESIII Collaboration), Phys. Rev. D **81**, 052005 (2010).
5. M. Ablikim *et al.* (BESIII Collaboration), Chin. Phys. C **34**, 4 (2010).
6. M. Ablikim *et al.* (BESIII Collaboration), Phys. Rev. Lett. **106**, 072002 (2011).
7. M. Ablikim *et al.* (BESIII Collaboration), Phys. Rev. D **83**, 012003 (2011).
8. M. Ablikim *et al.* (BESIII Collaboration), Phys. Rev. D **83**, 012006 (2011).
9. M. Ablikim *et al.* (BESIII Collaboration), Phys. Rev. D **83**, 032003 (2011).
10. M. Ablikim *et al.* (BESIII Collaboration), Phys. Rev. D **83**, 112005 (2011).

11. M. Ablikim *et al.* (BESIII Collaboration), Phys. Rev. Lett. **107**, 092001 (2011).
12. M. Ablikim *et al.* (BESIII Collaboration), Phys. Rev. Lett. **108**, 112003 (2012).
13. PDG 2010: Particle Data Group, Journal of Physics **G 37**, 075021 (2010).
14. E. Eichten, K. Gottfried, T. Kinoshita, K. D. Lane and T.-M. Yan, Phys. Rev. **D17**, 3090 (1978).
15. B. Aubert *et al.* (Babar Collaboration), Phys. Rev. **D 78**, 012006 (2008).
16. M. Ablikim *et al.* (BESII Collaboration) Phys. Rev. Lett. **95**, 262001 (2005).
17. G. J. Ding and M. L. Yan, Phys. Rev. **C 72**, 015208 (2005).
18. G. J. Ding and M. L. Yan, Eur. Phys. J. **A 28**, 351 (2006).
19. B. A. Li, Phys. Rev. D **74**, 034019 (2006).
20. T. Huang and S. L. Zhu, Phys. Rev. D **73**, 014023 (2006).